Hole nucleation in free-standing polymer membranes: the effects of varying molecular architecture

Andrew B. Croll† and Kari Dalnoki-Veress*

Received 14th April 2010, Accepted 23rd July 2010
DOI: 10.1039/c0sm00253d

Free-standing liquid films are generally unstable, failing whenever a hole or pore is created. The same is true of a polymer melt, although the details of the instability can be more complex and dependent on molecular architecture. Here, we compare the nucleation of holes in homopolymer films and films made from diblock co-polymers that can order into a cylindrical or lamellar phase. The different degrees of internal order (no long-range order, lamellar order, cylindrical order) has significant effects on the rate of hole formation. We find that lamellar order decreases the rate of film rupture by at least two orders of magnitude when compared to isotropic films. The hole formation is well described by a classical nucleation process. Notably, we find that the barrier to hole formation is identical for all samples studied here, favouring a simple capillary model. The vast differences in stability between films of differing internal structure is entirely quantified by the "attempt frequency" of barrier penetration and not the free energy barrier itself.

1 Introduction

If a simple liquid film such as water is made to freely span some region (for example, a bubble near a water surface) it is well known to be unstable, rupturing and collapsing almost instantly. A surfactant can be added which lowers the surface tension of the liquid layer and extends the lifetime of a bubble. In this case the film is stabilised through the Marangoni effect: if the film stretches (exposing more water to the air) the surface tension is increased, which opposes further stretching.[1–3] When the film is allowed to thin further and the surfactant is sufficiently large (for example a phospholipid), a 'black' film, much thinner than the wavelength of light, can be formed.[1–3] This lamellar state has a thickness that is on the order of two molecular layers and is stabilised simply by the energetic cost of exposing the lipid tail to the surrounding phase. Ultimately, such films are metastable and still doomed to failure: any small puncture will cause the top and bottom surfaces to connect and surface tension will drive hole growth eventually collapsing the film. This simple physical picture creates an attractive starting point for attempts to understand many processes relevant to living cells (vesicle fusion, pore opening, *etc.*) and is therefore receiving much attention in the literature.[4–9]

The increased interest in hole formation has also lead to the development of useful analogs of bio-membranes, for example synthetic materials such as diblock copolymers where the thickness and chemistry can be easily varied.[10–12] Diblock copolymers are linear polymers made up of two different blocks of repeating molecular units. Because the blocks are chemically distinct, a diblock copolymer melt can be found in one of two states – a homogeneous (disordered) blend or a microphase separated state. Higher temperatures (or shorter molecules) favour the higher entropy homogenous mixture, whereas at low temperature (or longer molecules) the enthalpic penalty of mixing the two chemically distinct blocks favours phase separation.[13,14] The phase separated state is complicated by the physical union of the two blocks, which results in the formation of self-assembled microphase separated structures. The particular structure is dictated primarily by the ratio of block lengths and can be understood simply from packing considerations. If the two blocks are similar in size, the diblock is symmetric and can form a lamellar ordered phase. As the asymmetry of the block length increases, there is a greater benefit to curve the interface and form a cylindrical structure with the shorter block in the middle. Increasing the asymmetry further enhances the curvature and favours the formation of spheres of the short block embedded in a matrix of the longer block (details are well described in[13,14]). This rich physics makes block copolymers ideal molecules for studies of membrane failure.[15] In particular, these molecules allow controlled studies in which different internal structure can be compared in films presenting identical surface energies.

A liquid film can be destabilised by different physical mechanisms, which can be generalised into two broad categories: nucleation driven or a spontaneous instability.[16–21] If a film is spontaneously unstable, any infinitesimal fluctuation of the surface will grow until it reaches the opposite surface and ruptures the film. This spontaneous instability, often termed *spinodal dewetting* because of its analogy to spinodal decomposition in phase separation, is generally characterised by a short timescale, and often associated with long range pattern formation. In particular, for a liquid film on a substrate, sinusoidal undulations of a particular wavelength, λ, form because of a balance between the van der Waals forces which can favour drawing the film surfaces together and the viscous loss associated with the movement of liquid from one region to another. A governing equation of motion can be written by considering the Navier–Stokes equation in the thin film limit. Linear stability

Department of Physics & Astronomy and the Brockhouse Institute for Materials Research, McMaster University, Hamilton, ON, Canada
† Current address: Department of Physics, North Dakota State University, Fargo, ND, USA. E-mail: andrew.croll@NDSU.edu

analysis yields predictions of the characteristic spacing of the resulting pattern and a characteristic time. In a rigidly supported film $\lambda \sim \gamma^{1/2}h^2/A^{1/2}$, where γ is the surface tension, h is the film thickness, and A is the Hamaker coefficient which characterises the strength of the van der Waals interaction. The fluctuations of the interface grow exponentially with time constant $\tau \sim \eta\gamma h^5/A^2$, where η is the film viscosity.[22–25]

If a film can resist spontaneous instability, for example if A is negative or if the film is so thick that the van der Waals forces cannot drive the instability on an experimental time scale, then the film can still fail through the thermal nucleation and growth of holes. In this regime a polymer film is in a metastable state – though ultimately the free energy is lowered once a hole can grow large enough, there is a nucleation barrier impeding the spontaneous destruction of the film. The free energy of a hole in a free-standing liquid film can most simply be written as,

$$F = -2\gamma\pi R^2 + \Gamma 2\pi R \quad (1)$$

where γ is the interfacial tension (note there are 2 surfaces), R is the radius of the hole, and Γ is an edge tension. In this simple capillary model, the energy is lowered by reducing the total surface area of the film (the first term), but because a film has some width there is also new surface created by opening a hole (the second term).[26–28] Notably, a critical hole size, R^*, must be created to overcome the energy barrier, F^*, given by

$$R^* = \Gamma/2\gamma \text{ and } F^* = \pi\Gamma^2/2\gamma \quad (2)$$

An alternate point of view more commonly found in the lipid-membrane literature considers the case where the surface energy is much smaller than the energy required to bend the interface such that a hole is formed.[4] In this case it is common to use the Helfrich free energy.[29] The cost of bending the interface for diblock copolymers is much less than that of lipid membranes, and for the homopolymer case the capillary model is reasonable, since the bending costs vanish. The use of the capillary model is less clear for the case of a diblock copolymer system where a stretching of the molecules is required to form the curvature at the rim of a hole. However, the additional cost of bending scales with the radius of the hole and can be included in the edge tension, Γ. Indeed, as we will see below, eqn (1) and (2) adequately describe the more complex cases of the anisotropic liquid film provided by the chain architecture of a diblock copolymer.

In the work presented here we directly measure the stability of thin, free-standing polymer films. We compare the nucleation rate of several different diblock copolymers with homopolymer of similar molecular weight. In particular, it is found that the rate of nucleation of holes, or pores, is intimately related to the molecular architecture: the nucleation rate is orders of magnitude lower in films of a symmetric diblock copolymer, which forms lamellae parallel to the film interfaces, than in films prepared from homopolymer or cylinder forming diblock copolymers of similar chain length.

2 Experimental

We have conducted measurements of hole nucleation in thin free-standing polymer films, of various architecture, by means of optical microscopy (see Fig. 1). Samples of the diblock copolymer polystyrene-poly(methyl methacrylate) (PS-PMMA), or polystyrene (PS) homopolymer were created by first spin-casting polymer from toluene solution onto freshly cleaved mica substrates (all polymer used as received from Polymer Source Inc., Montreal, Canada). Samples were typically annealed to drive off any residual solvent, equilibrate the molecular conformations in the thin films, and to ensure the formation of long ranged order resulting from microphase separation. Care is taken to anneal the polymer for long times in order to avoid any of the complexity associated with non-equilibrium chain conformations and entanglements.[30] The samples were annealed in vacuum at 160 °C for at least 4 h. Some copolymer films were not annealed after spin-casting and used "as cast", where the molecules are in a more disordered non-equilibrium state.

Films were floated on a clean water surface (Milli-Q) and lifted off the water such that they span a hole in a washer. A simple metal washer with a 4 mm hole has been used for such samples.[31] However, when studying nucleation, the rupture of the films is often initiated at the metal edge. We avoid this problem by using a perforated, thicker (hundreds of nm's) high molecular weight PS film (an ideal hole in the PS film can easily be made by using a hot probe near the surface and initiating the formation of a hole in the centre of the thick film). Such a substrate creates a 'liquid washer' since PS is in the melt state under our experimental conditions (see the schematic in Fig. 1a). However, owing to the very high molecular weight of the PS support, the washer can be considered solid-like due to its high viscosity and large thickness

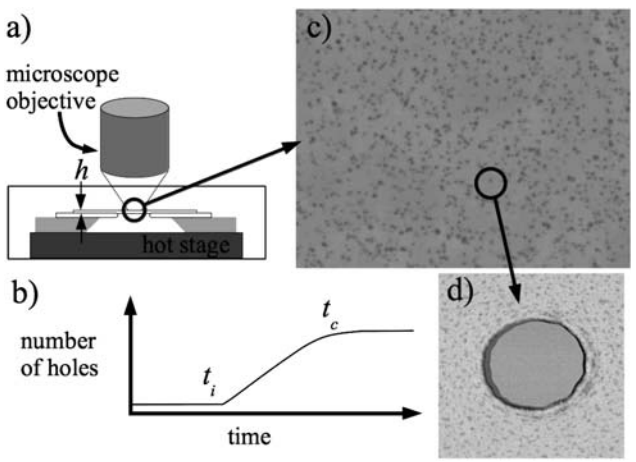

Fig. 1 a) A schematic of the experimental setup to probe the nucleation of holes. The film of interest with thickness, h, is placed on a thick polystyrene film with a hole, which in turn is supported on a stainless steel washer (see text for details). b) Schematic representation of the data that is obtained. For times less than t_i, holes are not yet big enough to be visible with optical microscopy. The holes grow, but after time t_c no further nucleation is observed. c) A representative optical microscope image of a cylinder forming diblock copolymer film (cyl-32k) with $h = 38$ nm (image width ~ 12 μm). Note that each dark spot correspond to a hole. d) Atomic force microscopy image of a single hole in a sample that was quenched to room temperature after time t_c (image width ~500 nm). The AFM image was taken with phase imaging under hard tapping conditions which creates contrast between the different domains of the diblock. In this AFM image the darker spots around the hole are due to the cylindrical PMMA domains.

on the time-scale of the experiments. We have verified that there is no influence on our experiments by comparing the rate of hole formation on a PS washer with that of films supported directly on a metal washer.

Two symmetric diblock copolymers were used with total number averaged molecular weights of 36.0 kg/mol and 42.0 kg/mol (lam-36k and lam-42k), and one asymmetric cylinder forming diblock with 31.5 kg/mol (cyl-32k). Details of the polymer systems used are given in Table 1. These diblock molecules allow the comparison of equilibrium (annealed) and non-equilibrium (as-cast) structures as well as lamellar and cylindrical order. In addition we also use a polystyrene homopolymer of molecular weight 93.2 kg/mol (hom-93k) for comparison to the simple isotropic liquid film case. The existence of order in the block copolymers can easily be verified with atomic force microscopy (AFM). As well as being of higher molecular weight, the homopolymer PS has a lower glass transition temperature than does the PMMA in the diblock used in this study (PS $\sim 97\,^{\circ}$C, PMMA $\sim 115\,^{\circ}$C). Both a change in glass transition and the lamellar structure can contribute to the hole nucleation rate. The disordered as-cast diblock films were used in an attempt to address these two issues and make a more direct comparison between well ordered samples and those that are less ordered. However, even the as-cast diblock films can pose a challenge to direct comparison due to their non-equilibrium nature. For this reason we include the cylinder forming block copolymer, which enables a more direct comparison between similar films (in chain length and glass transition) that have different internal structures (none, lamellar, or cylindrical).

Fig. 1 illustrates how a typical experiment is carried out. A film is placed on a hot stage (Linkam Scientific Instruments, UK) raised quickly to a temperature above its glass transition and observed with optical microscopy. Over some initial time period $t < t_i$ holes nucleate, but are not yet visible with the optical microscope. Once holes become visible the number of holes grows for some time. During the initial period of hole nucleation the nucleation rate is constant as is clear from Fig. 2. From the initial slope of the plot of the number of holes as a function of time the nucleation rate, N, is easily determined. After some time, $t \sim t_c$, the nucleation rate decreases and eventually the number of holes remains constant for two reasons. First of all as holes appear, the film thickens and the nucleation rate decreases. Secondly, as is clear from the optical image (see Fig. 1c) there are so many holes that they start to coalesce and the rate at which holes appear becomes comparable to the rate at which the holes coalesce. Regardless, the initial rise in the number of holes provides a robust measure of the nucleation rate, N.

Table 1 Polymer details: the number averaged molecular weights for the PS and PMMA blocks, the polydispersity index, the microstructural state and label used in the text

M_N^{PS} (kg/mol)	M_N^{PMMA} (kg/mol)	PI	Phase and label
93.2	0	1.04	Disordered – hom-93k
18.0	18.0	1.07	Lamellae – lam-36k
21.0	21.0	1.07	Lamellae – lam-42k
21.5	10.0	1.06	Cylinder – cyl-32k

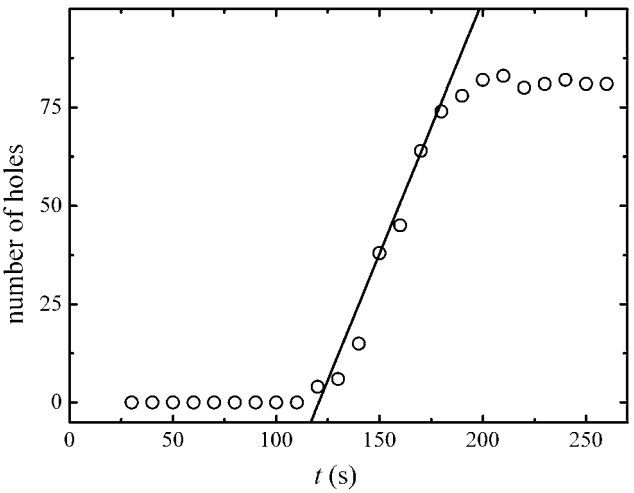

Fig. 2 A typical plot of the number of holes observed with optical microscopy as a function of time. In this particular experiment a film of ordered 42 kg/mol, lamellar forming diblock copolymer (lam-42k) with $h = 42$ nm is shown. For this molecular weight this thickness represents 1.5 bilayers (the film surface is flat). Here the onset of nucleation is observed at $t_i \sim 125$ s, and the slope of the line provides the initial nucleation rate, $N = 1.1 \pm 0.2$ holes/s.

3 Results and discussion

3.1 Spontaneous instability

Pattern formation can enable a simple method of differentiation between the two regimes of film failure (spontaneous or nucleated).[17,19,22] Fig. 3 shows AFM micrographs for several different films used in our experiments. These films are all approximately 40 nm thick and we note that there is no long range surface undulations (pattern) observed. In fact, the roughness in pre- and post- hole nucleation samples is experimentally indistinguishable. We further verify the lack of any long range order by computing two point correlation functions for several optical microscope images of very thin samples ($h \sim 20$ nm) that have undergone hole formation.[19] Within experimental error, we cannot observe any correlation of hole position. A second more important observation is that holes do not suddenly appear at one characteristic time, but appear slowly over the course of the experiment. Taken together these observations strongly suggest that the holes are nucleation driven and that the films are not spontaneously unstable.

It is important to note that the lack of pattern formation observed in these free-standing polymer films is not unexpected. For free-standing films, the velocity profile in the film normal direction is uniform resulting in plug flow.[32] This is in contrast with the velocity gradients which lead to viscous losses in a supported film (parabolic Poiseuille velocity profile). Since there is no mechanism to limit long wavelengths, there is no optimal undulation of the surface that emerges.[22,23] A calculation that considers this geometry within the framework of a polymer film on a liquid substrate leads to the same result – no selection of a wavelength – if the substrate's viscosity goes to zero.[33,34]

In contrast with samples that are spontaneously unstable, the strength of the van der Waals forces, characterised by the

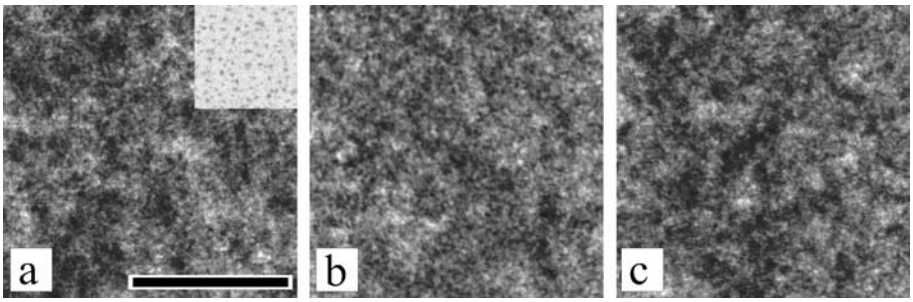

Fig. 3 Atomic force microscopy images of several block copolymer films used in this study. a) A cylinder forming film (the inset shows a corresponding section of AFM phase image which highlights the different domains of the diblock) b) An "as cast" film of 36 kg/mol diblock (lam-36k). c) Same system as b) but after annealing into the well ordered state. All films have a similar roughness, and no long range correlated fluctuations before or after an experiment could be seen. The size bar indicates 500 nm, and the RMS roughness is ~2 nm.

Hamaker coefficient, A, are not sufficient for the all films studied to drive the instability spontaneously. However, they are present. For the symmetric geometry of a free-standing film (air-sample-air), the van der Waals interaction will always favour bringing the two interfaces closer to one-another.[35] This additional interaction favours hole formation, and can be thought of as the disjoining pressure, $\Pi_{VDW} = A/6\pi h^3$, which will contribute to the free energy as an effective surface tension, $\gamma_{eff} = \gamma + \int_{\infty}^{h} \Pi \partial h$.[3,35] Since the effects of the van der Waals forces are already included in eqn (1) and (2) through the surface tension, they need not be treated separately.

3.2 Critical radius

Once a hole forms in a free-standing polymer film it will grow exponentially as,

$$R = R_0 \exp(t/\tau) \tag{3}$$

where R_0 is the initial hole size and τ is a time constant.[31,32] The radius of a hole in a diblock copolymer film also follows an exponential form, although the apparent time constant is significantly reduced when compared with a homopolymer film of similar thickness.[36] The exponential growth allows an estimate of the two times measured in our experiments. The time for the first hole to become visible, t_i, is simply the time for a hole to nucleate and grow to an observable size. If the nucleation rate is high then some holes form almost instantly upon heating (which is often the case for the thin films we have studied). For the high nucleation rate the time window of the experiment is dominated by the growth of the hole and at $t = 0$ the hole grows from its critical radius, R^*. Eqn (3) can be rewritten as,

$$t_i \sim \tau \ln(R_v/R^*) \tag{4}$$

where R_v is the size of a hole when it first becomes visible. Fig. 4 shows data from ordered and "as cast" block copolymer films, as well as polystyrene films at several temperatures. The growth of holes is observed with optical microscopy and the time constant, τ, is obtained directly in each sample by measuring the area of a hole as a function of time and fitting to eqn (3). The time at which a hole is first observed, t_i, is simply obtained by following the sequence of hole formation backwards in time and noting the time at which the first hint of a hole can be seen (*i.e.* the observation of the first pixel to change intensity). The solid line in Fig. 4 is a fit to eqn (4). We note that the excellent fit to the data is not only a verification of eqn (4) but also provides a measure of the critical hole size. Remarkably, the fact that all data sets are fit by the same equation implies that R^* *is independent of the molecular architecture* (homopolymer, ordered diblock, as-cast diblock). From the fit to the data, $R_v/R^* = 2.1$ and with $R_v \sim 400$ nm (the size of a single pixel with our microscope), we find $R^* \sim 50$ nm. For the capillary model the critical hole size is given by eqn (2). The edge tension can be estimated as the cost of the new surface created at the hole edge, $\Gamma = c\gamma h$, with c a geometric factor of order unity. Thus eqn (2) becomes,

$$R^* = ch/2 \text{ and } F^* = \pi\gamma c^2 h^2/2. \tag{5}$$

The simple estimate gives $R^* \sim 20$ nm, which is in excellent agreement with our observations.

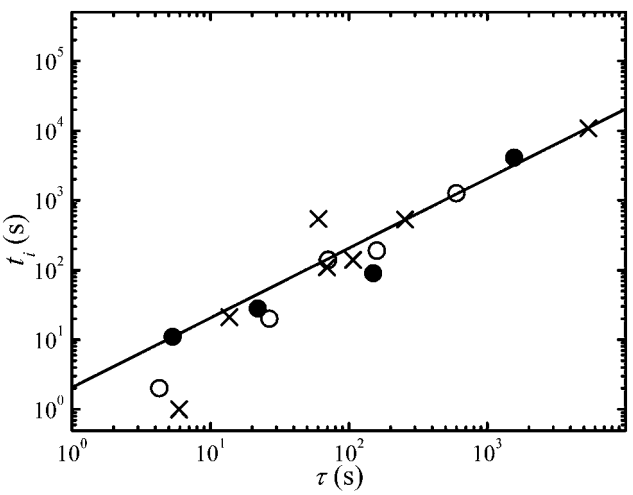

Fig. 4 The time of the first observed hole, t_i (obtained from plots like that shown in Fig. 2), as a function of the time constant of the exponential hole growth, τ. The open circles are disordered block copolymer (lam-42k), crosses are the same system in the ordered state (lam-42k), solid circles are polystyrene homopolymer (hom-93k)and the solid line is a fit to the theory described in the text given by eqn (4).

3.3 Nucleation and growth

The nucleation of the holes can be analyzed in terms of a classical energy barrier problem described by the Boltzmann equation,

$$N = a\exp\left(-\frac{F^*}{kT}\right) = a\exp\left(-\frac{\pi\gamma c^2 h^2}{2kT}\right) \quad (6)$$

where a is the attempt frequency, k is the Boltzmann constant, T is temperature, and the free energy barrier can be estimated using eqn (5). Fig. 5 shows the nucleation rates, obtained from the slope of Fig. 2, plotted as a function of temperature for four types of samples (homopolymer, ordered cylinder forming diblock, ordered lamellae forming diblock, as-cast symmetric diblock) suggested by the scaling in eqn (6). Several remarkable conclusions can be drawn: 1) nucleation clearly varies exponentially with inverse temperature for all the sample types explored; 2) within experimental uncertainties *all* molecular architectures have the same slope on this plot, indicating that the critical free energy barrier F^* is independent of the molecular architecture; and lastly, 3) only the attempt frequency is different for the various samples. It is found that the attempt frequency is highest for PS homopolymer, lower for the as-cast symmetric diblock and the ordered cylinder forming diblock, and lowest for ordered lamellar diblock copolymer. Evidently it is in the attempt frequency that the molecular details are manifested.

The data shown in Fig. 5 is well described by the classical nucleation eqn (6) which results in $F^*/k = 5.8 \times 10^4$ K or an energy barrier of $\sim 10^{-18}$ J. The capillary model suggests a free energy barrier given by eqn (5). Since PS and PS-PMMA have very similar surface energies, the edge tension will be the same resulting in the same free energy barrier. Quantitatively, the capilliary model predicts a barrier of approximately 10^{-16} J (taking the surface tension for PS and PMMA to be $\gamma = 34$ mN/m). While this is notably different from that measured experimentally, the simple capillary does not explicitly take into account the details of the van der Waals forces as the thickness decreases. Clearly, a more detailed theoretical model is required to achieve more than a simple scaling understanding of nucleation.

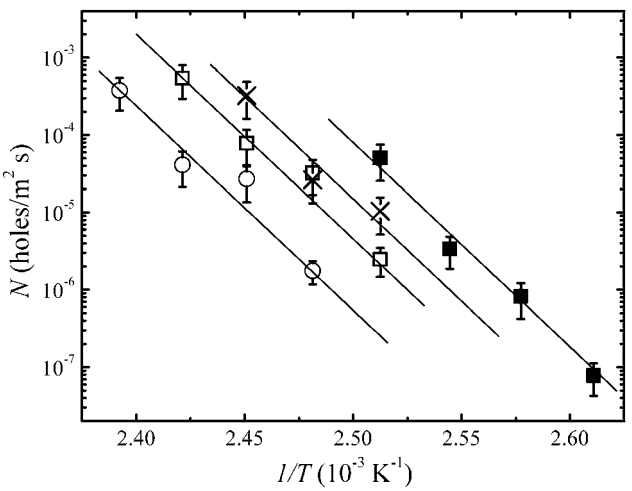

Fig. 5 Nucleation rate as a function of the inverse temperature for films with $h \sim 40$ nm. Open circles are well ordered symmetric diblock films (lam-42k), open squares are the same molecules in a disordered "as-cast" state. Black crosses are ordered cylinder forming diblock films (cyl-32k). The solid squares are the PS homopolymer films (hom-93k). Lines drawn to guide the eye.

Defects, like dirt in the sample, could 'unnaturally' lower the energy barrier. However, samples were created at different times, with different polymers, and with great care. It is unlikely that such defects would replicate the same free energy barrier over many experimental repetitions. Given the reasonable quantitative agreement between our measurement of R^* and the simple theory, defect driven nucleation is even less likely. The difference between the measured and observed free energy barrier may result from a surface energy that is different from the bulk due to presence of a disjoining pressure in the thin films.

In order to further test the capillary model we investigated hole nucleation in a series of ordered lamellae forming diblock films and homopolymer PS films of different thickness. The use of the ordered diblock system for a range of thickness causes an additional complexity most easily described by a simple example. Consider a film uniform in thickness after spincoating, with initial thickness such that it is somewhat thicker than a single lamellae. Upon ordering this film must form some regions with one lamella and some with two lamellae such that volume is conserved. In general, we can take the initial film thickness, $h = bL + \delta L$, where b is some integer, L is the thickness of a lamellar layer, and $0 < \delta < 1$. In that case, the surface is broken into islands if $\delta < 0.5$, holes if $\delta > 0.5$, or an interconnected structure if $\delta \sim 0.5$.[37–39] In order to make a direct comparison between the diblock films and homopolymer films, one must take into account the commensurability of the bilayers. The probability of nucleation in the thinner regions of the ordered diblock film, with $h = bL$, is so much more likely than in the region with $h = (b + 1)L$, that we can take the effective area of the film to be just that of the thinner region. For example in a film with $\delta = 0.5$, the nucleation rate per unit area is equal to that of a film bL thick with half the total film area.

Fig. 6 shows a plot of $\log(N)$ as a function of h^2 as suggested by eqn (6) for homopolymer and symmetric diblock films (hom-93k and lam-36k). For the lamellae forming diblock films the area is appropriately normalised to that of the thinnest regions as discussed above. In order to examine the same range of thicknesses the homopolymer films were nucleated at 120 °C, while the diblock films were nucleated at 135 °C. The data is again well fit by eqn (6) with a "slope" prefactor of -1.7×10^{15} m^{-2}. This corresponds to an energy barrier of 1.5×10^{-20} J for a 40 nm thick film. Though the results are in qualitative agreement with eqn (6), the value of the free energy barrier is lower than that obtained with the previous value from Fig. 5. This difference suggests again that the free energy of the capillary model as given in eqn (1) only captures the general scaling but the prefactor, a, in eqn (6) must contain some thickness dependence. The measurement of nucleation as a function of film thickness once again reveals that the homopolymer and symmetric diblock copolymer samples have similar energy barriers, while a difference in attempt frequency is observed.

3.4 Direct comparison

From the measurements that have been performed, it is clear that within the experimental errors, the energy barrier to nucleation in the films is identical and the difference in chain architecture is

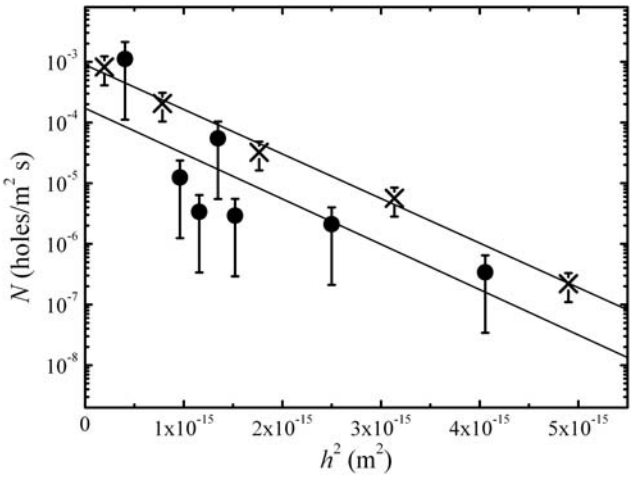

Fig. 6 Nucleation rate as a function of film thickness squared for homopolymer PS at $T = 120$ °C and a symmetric diblock at $T = 135$ °C. Crosses are for well ordered diblock films (lam-36k) and circles are for the homopolymer PS (hom-93k). The data of the block copolymer samples have been normalized to the amount of surface area corresponding to the thinnest portion of films. The larger scatter in the PS sample is due to a lower total number of holes per sample, and hence the weaker statistics illustrated with the larger error bars. The fit lines correspond to the scaling provided by eqn (6).

apparent in the magnitude of the attempt frequency only. In Fig. 7 we show the central result of this work, the nucleation rate of all samples at a thickness of 40 nm and temperature of 135 °C. In order to show data from all molecules at this temperature we are forced to extrapolate the data from lower temperatures for the polystyrene sample. We find that the lamellar block copolymer is two orders of magnitude more stable than the homopolymer, and an order of magnitude more stable than the cylindrical geometry diblock and disordered films of similar molecular weight. As might be expected, the increased stability also scales with molecular weight, evident when comparing the two lamellar block copolymers studied here. This final observation allows us to conclude that hole formation is hindered in diblock copolymer films simply because the attempt frequency is modified by the layered structure. For a hole to form, fluctuations in film thickness must occur. We speculate that the lamellar films resists local thickness variations because this requires extra stretching of the polymer chains, thus decreasing the attempt frequency. A hole can 'fluctuate' into existence if some polymer chains migrate to the film surface, something that is energetically unfavourable.[36,40] The results obtained indicate that because of the depression of the attempt frequency in the layered films, remarkably stable liquid films can be prepared.

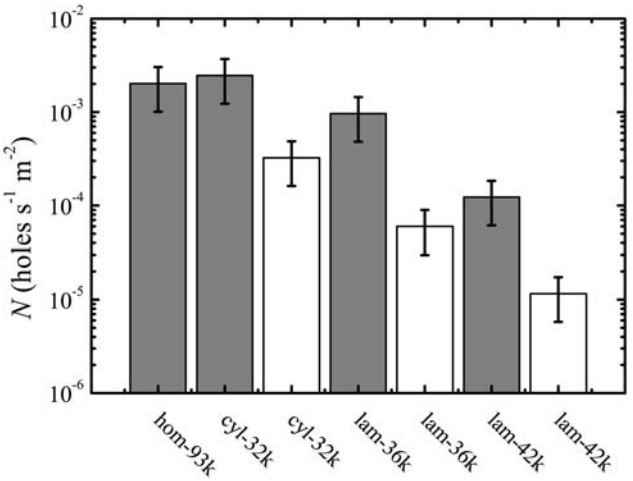

Fig. 7 Nucleation rate of thin polymer films with $h \sim 40$ nm and at $T = 135$ °C of varying molecular architecture and degrees of order shown on a logarithmic scale. Homopolymer and the "as-cast" less-ordered block copolymer are shown by grey bars. Ordered copolymer is shown with white bars. Note that ordered samples have lower nucleation rates in all cases when compared to the "as-cast" or isotropic homopolymer case. The total molecular weight and polymer architecture is indicated in brackets (see Table 1 for meaning of labels).

4 Conclusions

We have shown the results of several measurements of the nucleation rate of holes in thin, free-standing polymer films. Various chain architectures have been investigated: homopolymer, cylinder forming diblock copolymer, and two lamellae forming diblock copolymers. These experiments clearly indicate a significant increase in the stability of ordered lamella forming block diblock films. Surprisingly we find that the barrier to nucleation is independent of the chain architecture, while the stability seems to be related to the internal structure of the liquid through a modified attempt frequency. The barrier to hole formation was measured in two different ways: through the dependence of nucleation on temperature and the dependence on film thickness. The results are well described by the simple capillary model. The effects of chain architecture (homopolymer and diblock) are found to only influence the attempt frequency, and not the barrier to nucleation itself. While we see remarkable agreement with the scaling predictions, quantitative agreement in the prefactors was not obtained suggesting that a more detailed molecular model is necessary in order to further understand the nucleation mechanism of membrane failure.

References

1 J. E. S. Johonnott, *Phil. Mag.*, 1906, **11**, 746–753.
2 M. Perrin, *Ann. Phys.*, 1918, **9**, 160–184.
3 V. Bergeron, *J. Phys.: Condens. Matter*, 1999, **11**, R215–R238.
4 R. Lipowsky, *Nature*, 1991, **349**, 475–481.
5 R. Bruinsma, M. Goulian and P. Pincus, *Biophys. J.*, 1994, **67**, 746–750.
6 O. Sandre, L. Moreaux and F. Brochard-Wyart, *Proc. Natl. Acad. Sci. U. S. A.*, 1999, **96**, 10591–10596.
7 L. Yang and H. Huang, *Science*, 2002, **297**, 1877–1879.
8 R. Jahn, T. Lang and T. Südhof, *Cell*, 2003, **112**, 519–533.
9 W. K. den Otter, *J. Chem. Phys.*, 2009, **131**, 205101.
10 B. Discher, Y.-Y. Won, D. Ege, J. C.-M. Lee, F. Bates, D. E. Discher and D. Hammer, *Science*, 1999, **284**, 1143–1146.
11 D. E. Discher and A. Eisenberg, *Science*, 2002, **297**, 967–973.
12 H. Bermudez, H. Aranda-Espinoza, D. Hammer and D. Discher, *Europhys. Lett.*, 2003, **64**, 550–556.
13 F. S. Bates and G. H. Fredrickson, *Annu. Rev. Phys. Chem.*, 1990, **41**, 525–557.
14 G. H. Fredrickson and F. S. Bates, *Annu. Rev. Mater. Sci.*, 1996, **26**, 501–550.
15 S. Joly, D. Ausserré, G. Brotons and Y. Gallot, *Eur. Phys. J. E*, 2002, **8**, 355–363.

16 F. E. C. Culick, *J. Appl. Phys.*, 1960, **31**, 1128–1129.
17 R. Seemann, S. Herminghaus and K. Jacobs, *Phys. Rev. Lett.*, 2001, **86**, 5534–5538.
18 G. Reiter, M. Hamieh, P. Damman, S. Sclavons, S. Gabriele, T. Vilmin and E. Raphaël, *Nat. Mater.*, 2005, **4**, 754–758.
19 K. Jacobs, S. Herminghaus and K. Mecke, *Langmuir*, 1998, **14**, 965–969.
20 T. Vilmin and E. Raphaël, *Eur. Phys. J.E.*, 2006, **94**, 1–14.
21 O. Bäumchen, R. Fetzer and K. Jacobs, *Phys. Rev. Lett.*, 2009, **103**, 247801.
22 A. Vrij, *Discuss. Faraday Soc.*, 1966, **42**, 23–33.
23 F. Wyart and J. Daillant, *Can. J. Phys.*, 1990, **68**, 1084–1088.
24 M. Sferrazza, M. Heppenstall-Butler, R. Cubitt, D. Bucknall, J. Webster and R. A. L. Jones, *Phys. Rev. Lett.*, 1998, **81**, 5173–5176.
25 R. Xie, A. Karim, J. F. Douglas, C. C. Han and R. A. Weiss, *Phys. Rev. Lett.*, 1998, **81**, 1251–1254.
26 C. Taupin, M. Dvolaitzky and C. Sauterey, *Biochemistry*, 1975, **14**, 4771–4775.
27 Litster, *Phys. Lett. A*, 1975, **53**, 193–194.
28 M. Elbaum and S. G. Lipson, *Phys. Rev. Lett.*, 1994, **72**, 3562–3565.
29 W. Helfrich, *Z. Naturforsch.*, 1973, **28C**, 693–703.
30 D. Podzimek, A. Saier, R. Seemann, K. Jacobs and S. Herminghaus, 2001, arXiv:cond-mat/0105065.
31 K. Dalnoki-Veress, B. Nickel, C. Roth and J. Dutcher, *Phys. Rev. E: Stat. Phys., Plasmas, Fluids, Relat. Interdiscip. Top.*, 1999, **59**, 2153–2156.
32 G. Debrégeas, P. Martin and F. Brochard-Wyart, *Phys. Rev. Lett.*, 1995, **75**, 3886.
33 F. Brochard-Wyart, P. Martin and C. Redon, *Langmuir*, 1993, **9**, 3682.
34 P. de Gennes, F. Brochard-Wyart and D. Quéré, *Capillarity and Wetting Phenomena*, Springer-Verlag, New York, 2002, pp. 154–190.
35 J. Israelachvili, *Intermolecular and surface forces*, Academic Press, London, 1991.
36 B. Croll, M. J. Farrar and K. Dalnoki-Veress, to be published.
37 G. Coulon, D. Ausserre and T. P. Russell, *J. Phys.*, 1990, **51**, 777–786.
38 G. Coulon, B. Collin, D. Ausserre, D. Chatenay and T. P. Russell, *J. Phys.*, 1990, **51**, 2801–2811.
39 P. Green and R. Limary, *Adv. Colloid Interface Sci.*, 2001, **94**, 53–81.
40 A. Croll, M. Matsen, A.-C. Shi and K. Dalnoki-Veress, *Eur. Phys. J. E*, 2008, **27**, 407–411.